博士論文

The role of Foxp2 in thalamic patterning during development

(発生期の視床パターン形成における **Foxp2** の役割)

蛭子　はるか

Table of Contents

Abstract	**3**
Introduction	**4**
Materials and Methods	**6**
Results	**12**
Discussion	**19**
Acknowledgment	**24**
References	**25**
Figures	**32**

Abstract

The molecular mechanisms underlying the formation of the thalamus during development have been investigated intensively. Although transcription factors distinguishing the thalamic primordium from adjacent brain structures have been uncovered, those involved in patterning inside the thalamus are largely unclear. Here I show that Foxp2, a member of the forkhead transcription factor family, regulates thalamic patterning during development. I found a graded expression pattern of Foxp2 in the thalamic primordium of the mouse embryo. The expression levels of Foxp2 were high in the posterior region and low in the anterior region of the thalamic primordium. In Foxp2 (R552H) knockin mice, which have a missense loss-of-function mutation in the forkhead domain of Foxp2, thalamic nuclei of the posterior region of the thalamus were shrunken, while those of the intermediate region were expanded. Consistently, thalamocortical projection patterns were changed in Foxp2 (R552H) knockin mice. My results uncovered important roles of Foxp2 in thalamic patterning and thalamocortical projections during development.

Introduction

The thalamus plays critical roles as a relay center of sensory information in the brain (Fig. 1*A*). Most sensory information is transmitted from the periphery to the primary sensory areas in the cerebral cortex through the thalamus, and the loss of thalamic functions results in severe sensory deficits [1]. The thalamus consists of many structurally and functionally segregated nuclei, which are thought to be structural bases of sensory information processing in the thalamus (Fig. 1*B*). For example, the ventral posterior nucleus (VP) of the thalamus conveys somatosensory information and sends its axons to the primary somatosensory area (S1) of the cerebral cortex.

Early in development, the thalamic primordium is distinguished from adjacent brain structures such as the prethalamus, the pretectum and the epithalamus. Then, the thalamic primordium differentiates into various thalamic nuclei such as the anterodorsal nucleus (AD), the anteroventral nucleus (AV), the posterior nucleus (Po) and the VP. This process leading to the formation of thalamic nuclei is called thalamic patterning. The AD and the AV are located in the anterior region of the thalamus, whereas the VP and the Po reside in the posterior region.

The mechanisms that distinguish the thalamic primordium from adjacent brain structures have been extensively examined [2]. Previous papers have uncovered transcription factors regulating the formation of the thalamic primordium [3-10]. The homeodomain transcription factor Otx2 is required for acquiring thalamic identity, and the lack of Otx2 results in the activation of markers of the pretectum [3]. The zinc finger transcription factors Fezf1 and Fezf2 are crucial for the formation of the prethalamus and the thalamus [7]. Irx3 and Pax6 are involved in creating the cellular competence necessary for the formation of the thalamus [4]. In contrast, transcription factors regulating patterning inside the thalamus are still largely unclear, even though recent pioneering studies uncovered several molecules expressed in specific subsets

of thalamic nuclei [11-14]. In this study, I focus on the transcriptional factor Forkhead box protein p2 (Foxp2).

The *FOXP2* gene was originally associated with a developmental verbal dyspraxia in a study that described a multigenerational pedigree (the KE family) in which all affected members inherited missense mutation (R553H) disturbing the DNA-binding domain of the encoded protein [15]. The protein encoded by *FOXP2* contains a glutamine-rich region, a zinc-finger motif, a leucine-zipper, a forkhead domain and an acidic C-terminus [16] and, according to previous reports, is considered to act as a repressor [17, 18]. Previous ChIP experiments identified direct targets of human FOXP2 in the developing brain and in neuronal cell lines [17, 18]. Foxp2 is a member of the forkhead transcription factor family. This family consists of more than 30 transcription factors, many of which play crucial roles in developmental processes [16, 19-23]. Therefore, it seems plausible that Foxp2 also plays important roles during development.

In the developing mouse brain, *Foxp2* is highly expressed in many regions such as the cerebral cortex, the striatum, the thalamus and the cerebellum [24], and the roles of Foxp2 have been intensively investigated in brain regions other than the thalamus. For example, knockdown of Foxp2 resulted in reduced spine density in Area X of the zebra finch, suggesting that Foxp2 regulates spine dynamics [25]. Foxp2 (R552H) knockin mice showed deficits in motor-skill learning, accompanied by abnormal synaptic plasticity in striatal and cerebellar neural circuits, suggesting that Foxp2 is also crucial for synaptic plasticity [26]. Moreover, Foxp2 knockout resulted in an absence of ultrasonic vocalization in mouse pups, suggesting a role of Foxp2 in social communication functions [23, 27]. Abnormalities of neuronal morphology were also observed in mice with disruptions in Foxp2 [23, 27]. During development, it was reported that Foxp2 increased neuronal differentiation in the embryonic forebrain and regulated neurite

outgrowth in primary neurons [28, 29]. The roles of Foxp2 in the developing thalamus, however, have not been elucidated. Here, I demonstrate that Foxp2 regulates thalamic patterning and thalamocortical projections during development.

Materials and Methods

Animals

ICR mice (*Mus musculus*) were purchased from SLC (Hamamatsu, Japan) and were reared on a normal 12 hr light/dark schedule. The day of insemination was designated as embryonic day 0 (E0), and the day of birth was defined as postnatal day 0 (P0). Foxp2 (R552H) knockin mice were described previously [23]. All procedures were performed in accordance with protocols approved by the University of Tokyo Animal Care Committee and the Kanazawa University Animal Care Committee. Experiments were repeated at least three times and gave consistent results.

Plasmids.

pCAG-EGFP and pCAG-mCherry were described previously [30]. A Foxp2-shRNA-expression vector (Foxp2 shRNA) was constructed using a pSUPER.basic vector (Oligoengine, Seattle, WA). The sequences used for shRNA experiments were designed using the web-based software siDIRECT (http://sidirect2.rnai.jp/) and are 5'- GCAGTTAACACTTAATGAA-3' against Foxp2, and 5'-CAACAAGATGAAGAGCACC-3' as non-targeting negative control.

Plasmids were purified using an Endofree plasmid Maxi kit (Qiagen, Germany). Prior to electroporation experiments, plasmid DNA was diluted to 1 mg/mL in TE, and Fast Green

solution was added at a final concentration of 0.03% to monitor the injection.

In utero *electroporation*

In utero electroporation was performed as described previously [31-33] with slight modifications. Briefly, pregnant ICR mice were anesthetized with sodium pentobarbital, and the uterine horns were exposed. Approximately 1–2 μl of DNA solution (1 mg/ml) was injected into the third ventricle of embryos at the indicated ages using a pulled glass micropipette. Each embryo within its uterus was placed between tweezer-type electrodes (CUY650 P0.5-3, NEPA Gene). Square electric pulses (30 V, 50 ms) were passed five times at 1 s intervals using an electroporator (ECM830, BTX). Care was taken to quickly place embryos back into the abdominal cavity to avoid excessive temperature loss. The wall and skin of the abdominal cavity were sutured, and embryos were allowed to develop normally.

In situ *hybridization*

In situ hybridization using digoxigenin-labeled RNA probes was performed as described previously [34, 35]. Briefly, sections prepared from fresh-frozen tissues were treated with 4% paraformaldehyde (PFA) in phosphate-buffered saline (PBS), and 0.25% acetic anhydride in triethanolamine (TEA). The sections were incubated overnight with digoxigenin-labeled RNA probes in hybridization buffer (50% formamide, 5× saline-sodium citrate buffer, 5× Denhardt's solution, 0.3 mg/ml yeast RNA, 0.1 mg/ml herring sperm DNA, and 1 mM dithiothreitol). The sections were then incubated with an alkaline phosphatase-conjugated anti-digoxigenin antibody (Roche) and were visualized using NBT/BCIP as substrates. In some experiments, the sections were then subjected to Hoechst 33342 staining and immunohistochemistry.

Probes used here were mouse *cadherin-6, Foxp2, calbindin 2, Lhx2, Gbx2* and *EphA8*.

Cadherin-6 and *Foxp2* probes were described previously [36, 37]. *Calbindin 2* and *Lhx2* cDNA fragments were purchased from RIKEN. *Gbx2* and *EphA8* cDNA fragments were amplified by RT-PCR and inserted into pBluescript vectors. The sequences of primers used to amplify the *Gbx2* and *EphA8* probes were GAGTCAAAGGTGGAAGATGACC / ACTGCTCTGCACTCAACTCAAA and CCTAGAGTGACAGAGGTCAGGC / CCCTGTTTTCCTGTTGAATAGC, respectively.

Immunohistochemistry

Immunohistochemistry was performed as described previously with slight modifications [30, 38]. Sections prepared from fresh-frozen tissues were fixed with 4% PFA/PBS, permeabilized with 0.1-0.5% Triton X-100/PBS, and incubated overnight with primary antibodies, which included rabbit anti-FOXP2 (Abcam), rabbit anti-FOXP2 (ATLAS) and rabbit anti-VGLUT2 (Synaptic Systems) antibodies. After incubation with secondary antibodies and Hoechst 33342, the sections were washed and mounted. Sections prepared from perfused tissues were also used. In some experiments, the sections were then subjected to fluorescent Nissl (Molecular Probes) and Hoechst 33342 staining. Epifluorescence microscopy was carried out with an Axioimager A1 microscope (Carl Zeiss, Germany) and a BZ-9000 microscope (KEYENCE, Japan). Confocal microscopy was performed with a FLUOVIEW FV10i (Olympus, Japan). Stereomicroscopy was performed with a MZ16F fluorescence stereomicroscope (Leica, Germany).

DiI tracing

To retrogradely label the soma of thalamic neurons projecting to the prefrontal cortex, P6 pups were anesthetized by cooling, and 0.1 μl of 10% DiI (D3911, Molecular Probes) in dimethylformamide (DMF) was injected into the prefrontal cortex with capillary micropipettes

hooked up to a Hamilton 1 μm syringe [39]. The pups were then perfused with 4% PFA at P7. Brains were isolated and fixed in 4% PFA overnight, and 50 μm sections were cut using a vibratome. The sections were subjected to Hoechst 33342 staining and immunohistochemistry. When sections were labeled with DiI, digitonin was used for permeabilization instead of Triton-X 100 because DiI signals tend to be better preserved after digitonin treatment than after Triton-X 100 treatment [40].

To retrogradely label the soma of thalamic neurons projecting to S1 of the cerebral cortex, P13 pups were anesthetized, and 0.1 μl of 10% DiI (D3911, Molecular Probes) in dimethylformamide (DMF) was injected into S1 with capillary micropipettes hooked up to a Hamilton 1 μm syringe [39]. The pups were then perfused with 4% PFA at P15. Brains were isolated and fixed in 4% PFA overnight, and 50 μm sections were cut using a vibratome. The sections were subjected to Hoechst 33342 staining and to immunohistochemistry using digitonin.

Quantification of the expression levels of Foxp2 immunohistochemistry.

Averaged densitometric scans were performed on three adjacent horizontal sections of the embryonic mouse thalamic primordium along the anterior-posterior axis of the thalamus. Briefly, images of Foxp2 immunohistochemistry were digitally acquired with a CCD camera (AxioCam, Zeiss). Using ImageJ software, background signal intensities were subtracted from the images using the rolling ball filter with a diameter of 200 pixels, and then the images were normalized so that each pixel value fell between 0 and 255. Densitometric profiles of Foxp2 signals within rectangular areas along the anterior-posterior axis of the thalamic primordium were generated using the line profile function of ImageJ.

To quantify the percentages of Foxp2-positive cells in the thalamic primordium, horizontal sections were stained with anti-FOXP2 antibody and Hoechst 33342. The background

signal intensities were defined as the averaged signal intensities of Foxp2-negative cells in the pretectum. After background signal intensity was subtracted from images, the number of Hoechst-positive cells with Foxp2 immunoreactivity was counted, and was divided by that of Hoechst-positive cells.

To quantify the expression levels of Foxp2 at a single cell level, horizontal sections were stained with anti-FOXP2 antibody and Hoechst 33342, and confocal microscopic images were analyzed using ImageJ software (National Institutes of Health). After background signal intensity was subtracted from images, the Foxp2 signal intensity in each Hoechst-positive nucleus in the thalamic primordium was measured.

Quantification of the sizes of thalamic nuclei.

Coronal sections were prepared from wild type and Foxp2 (R552H) knockin mice at P2, and *in situ* hybridization was performed to visualize thalamic nuclei. The VP and the Pf were identified with the expression patterns of Cad6 and EphA8, respectively. The intermediate region of the thalamus was identified with Lhx2 expression patterns. Images were taken using a Leica stereomicroscope and analyzed using NIH image software (National Institute of Health).

To quantify the size of the VP, coronal sections located more posterior to the section with the largest LGN were selected. Among these sections, a section containing the largest size of VP was used for quantification. The periphery of the VP labeled with Cad6 was extracted manually and blindly, and the area of the VP was measured.

To quantify the size of the Pf, coronal sections located more posterior to the section with the largest LGN were selected. Among these sections, a section containing the largest size of Pf was used for quantification. The periphery of the Pf labeled with EphA8 was extracted manually and blindly, and the area of the Pf was measured.

To quantify the size of the intermediate region of the thalamus, a section located 200 – 250 μm posterior to the section with the largest LGN was used. The periphery of the intermediate region labeled with Lhx2 was extracted manually and blindly, and the area of the intermediate region was measured.

Quantification of the location of DiI-injected site in the prefrontal cortex.

Pictures of the dorsal views of brains of wild type and Foxp2 (R552H) knockin mice were taken using an MZ16F fluorescence stereomicroscope and analyzed using NIH image software (National Institute of Health). To each picture, I applied a rectangular coordinate system in a two-dimensional plane as follows. First, I defined the y-axis as a line passing through the midline in an anteroposterior direction, and the points at which y=0 and y=1 were defined as the places corresponding to the most caudal point and the most rostral point of the cortical hemisphere, respectively. The x-axis was drawn perpendicular to the y-axis, and the point at which x=0 corresponded to the midline, while the point at which x=1 corresponded to the most lateral point of the injected cortical hemisphere. I then measured coordinates of the location of DiI injection sites.

Quantification of the sizes of the DiI-positive region in the thalamus of mice injected with DiI into the prefrontal cortex.

Coronal sections were prepared from wild type and Foxp2 (R552H) knockin mice that were injected with DiI into the prefrontal cortex, and stained with anti-VGLUT2 antibody using digitonin. Images were taken using an Axioimager A1 microscope and analyzed using NIH image software (National Institute of Health). In each animal, a section containing the largest size of the VP was used for quantification. Because the intensities of DiI signals varied among

animals, images were thresholded manually to remove background signal intensities. For each section, the areas with signal intensities greater than the threshold signal intensity were measured, and their total area was divided by the area of the thalamus.

Quantification of the sizes of the DiI-positive regions in the thalamus of mice injected with DiI into the primary somatosensory area.

Coronal sections were prepared from wild type and Foxp2 (R552H) knockin mice that were injected with DiI into S1 of the cerebral cortex, and stained with anti-VGLUT2 antibody using digitonin. Images were taken using a BZ-9000 microscope and analyzed using NIH image software (National Institute of Health). In each animal, a section containing the largest size of the VP was used for quantification. The peripheries of the DiI-positive/VGLUT2-negative region and the DiI-positive/VGLUT2-positive region were extracted manually, and the areas of the DiI-positive regions were measured. The area of the DiI-positive/VGLUT2-negative region was then divided by that of the DiI-positive/VGLUT2-positive region.

Results

The expression pattern of Foxp2 in the thalamic primordium of the mouse embryo

It was reported that thalamic nuclei are unclear at embryonic day 12.5 (E12.5) and are distinguishable by E16.5 [11]. I therefore examined the expression pattern of Foxp2 protein in horizontal sections of the thalamic primordium at E14.5 using immunohistochemistry (Fig. 2*A*). I used anti-FOXP2 antibody whose specificity we had previously confirmed [37] and found a graded expression pattern of Foxp2 in the thalamic primordium (Fig. 2*B*). Foxp2 expression

levels were highest in the posterior region (Fig. 2*B*, arrowhead), lower in the intermediate region, and lowest in the anterior region of the thalamic primordium (Fig. 2*B*). Consistently, my quantification showed gradual changes in Foxp2 expression levels in the thalamic primordium (Fig. 2*G*). Another anti-FOXP2 antibody gave similar results (Fig. 3*A*). Sagittal sections also showed a graded expression pattern of Foxp2 (Fig. 2*D*,*E*). I next examined the expression pattern of *Foxp2* mRNA using *in situ* hybridization. Consistent with the expression pattern of Foxp2 protein, *Foxp2* mRNA was abundant in the posterior region (Fig. 2*C*,*F*, arrowheads) and almost absent in the anterior region of the thalamic primordium (Fig. 2*C*,*F*), which was consistent with a recent report examining the mRNA expression patterns of various molecules in the developing thalamus [41].

This graded expression pattern of Foxp2 in the thalamic primordium could be explained by two possible mechanisms. The first possibility was that the expression level of Foxp2 in each cell was indeed low in the anterior region and high in the posterior region. Alternatively, it was also possible that the number of Foxp2-positive cells was smaller in the anterior region than in the posterior region, and as a result, Foxp2 expression levels appeared lower in the anterior region macroscopically. To distinguish these two possibilities, I quantified the percentages of Hoechst-positive cells with Foxp2 signals in the thalamic primordium at E14.5. I found that almost all the cells were Foxp2-positive in both anterior and posterior regions of the thalamic primordium (Fig. 2*I*), suggesting that Foxp2 signal intensity in each cell rather than the number of Foxp2-positive cells was smaller in the anterior region of the thalamic primordium. Consistently, when I quantified the expression levels of Foxp2 at a level of single cells, I found that Foxp2 signal intensity in each cell in the anterior region was indeed significantly lower than that in the posterior region of the thalamic primordium (Fig. 2*H*,*J*,*K*). I therefore concluded that the expression levels of Foxp2 in the anterior region are lower than those in the posterior region of

the thalamic primordium. These results indicate that Foxp2 has a graded expression pattern in the thalamic primordium during embryonic development, and that the graded expression of Foxp2 is achieved, at least partially, at the level of mRNA because the graded expression patterns of Foxp2 were detected by *in situ* hybridization (Fig. 2*C*,*F*).

I next examined the expression patterns of Foxp2 in the developing thalamus at different time points. Horizontal sections of the thalamic primordium at E12 and P2 were stained with anti-FOXP2 antibody. Similar to sections at E14, sections at E12 showed graded expression patterns in the thalamic primordium. Interestingly, at P2, when thalamic patterning has almost finished, the graded expression pattern of Foxp2 in the thalamus was lost, and Foxp2 expression remained in some thalamic nuclei (Fig. 3*B*). These results suggest that graded expression patterns are present when thalamic patterning proceeds.

The role of Foxp2 in thalamic patterning during development

The graded expression pattern of Foxp2 led me to hypothesize that Foxp2 plays an important role in thalamic patterning during development (Fig. 4). To examine the role of Foxp2 in thalamic patterning, I utilized Foxp2 (R552H) knockin mice that have a missense loss-of-function mutation in the forkhead domain of Foxp2 (Fig. 5) [23, 26]. This mutation corresponds to a human FOXP2 (R553H) mutation in human FOXP2, and disrupts the DNA binding and transactivation properties of FOXP2 protein [42, 43]. I conducted VGLUT2 immunohistochemistry using horizontal sections of the thalamus of Foxp2 (R552H) knockin mice at postnatal day 7 (P7) (Fig. 6*A*). I found that the VP of the thalamus, which was reported to express VGLUT2 [44], was markedly smaller in Foxp2 (R552H) knockin mice than in wild-type control mice (Fig. 6*B*, arrowheads), suggesting that Foxp2 is required for the formation of the VP during development.

Because the VP is located in the posterior region of the thalamus, it seemed plausible that Foxp2 is important for the formation of not only the VP but also other thalamic nuclei located in the posterior region of the thalamus. Because it was difficult to distinguish other thalamic nuclei using anti-VGLUT2 antibody, I examined the expression patterns of molecular markers that are expressed in specific subsets of nuclei in the thalamus, including *EphA8, calbindin 2* and *cadherin-6*, using coronal sections (Fig. 7*A*). *EphA8*, *calbindin 2* and *cadherin-6* are expressed in the parafascicular nucleus (Pf), the posterior nucleus (Po) and the VP, respectively, in the posterior region of the thalamus [13, 14, 45] (Fig. 7*A*, blue nuclei). I found that *EphA8*- and *calbindin 2*-positive areas were significantly smaller in the posterior region of the thalamus in Foxp2 (R552H) knockin mice (Figs. 7*B, 7E* and 8, arrows), suggesting that Foxp2 is required for the formation of the Po and the Pf. *Cadherin-6*-positive areas were also markedly smaller in Foxp2 (R552H) knockin mice (Figs. 7*B, 7E* and 8, arrows), suggesting that Foxp2 is also required for the formation of the VP. This finding is consistent with the result obtained by VGLUT2 immunostaining (Fig. 6). These results suggest that Foxp2 is required for the formation of thalamic nuclei located in the posterior region of the thalamus.

Given that thalamic nuclei of the posterior region were smaller in Foxp2 (R552H) knockin mice, it seemed possible that those thalamic nuclei changed their identities to different thalamic nuclei. I therefore examined the distribution patterns of markers expressed in the intermediate region of the thalamus, such as *Gbx2* and *Lhx2*, at P2 [11, 14] (Fig. 7*A*, yellow nuclei). As expected, I found that *Gbx2*- and *Lhx2*-positive areas were significantly larger in Foxp2 (R552H) knockin mice than in wild-type mice (Figs. 7*C, 7E* and 8), suggesting that thalamic nuclei in the intermediate region of the thalamus were expanded in Foxp2 (R552H) knockin mice. In contrast, markers of the anterior region of the thalamus (Fig. 7*A*, red nuclei) were not affected in Foxp2 (R552H) knockin mice (Fig. 7*D*). These results suggest that the

posterior region of the thalamus obtained the properties of the intermediate region. Taken together, these results indicate that Foxp2 regulates fate determination in the thalamus during development.

In addition to the expression patterns of molecular markers, it seemed possible that cytoarchitectonic structures of thalamic nuclei were also affected in Foxp2 (R552H) knockin mice. I therefore conducted Nissl staining using coronal sections of the thalamus of Foxp2 (R552H) knockin mice at P7 (Fig. 9). I found that borders between thalamic nuclei were obscure in the thalamus of Foxp2 (R552H) knockin mice compared with those of wild type mice. These results suggest that Foxp2 is required for the formation of cytoarchitectonic structures of thalamic nuclei.

Foxp2 in the thalamus regulates thalamic patterning autonomously

Because Foxp2 is expressed not only in the thalamus but also in other brain regions such as the cerebral cortex and the striatum, and because I used Foxp2 (R552H) global knockin mice for the analysis of thalamic patterning, it remained possible that changes in thalamic patterning were mediated by Foxp2 expressed in the other brain regions. I thus examined whether Foxp2 in the thalamus was important for thalamic patterning using *in utero* electroporation (Fig. 10*A*). First, to suppress Foxp2 expression, I designed a Foxp2-shRNA-expression vector (Foxp2 shRNA) and introduced the Foxp2 shRNA into the thalamus using *in utero* electroporation at E11. Using Foxp2 immunohistochemistry, I found that the Foxp2 shRNA effectively suppressed Foxp2 expression in the thalamus at E14 (Fig. 10*C*). I confirmed that there were no transfected cells in the cerebral cortex (Fig. 10*B*), suggesting that Foxp2 shRNA is selectively introduced in the thalamus. To examine if introducing Foxp2 shRNA into the thalamic primordium affects thalamic patterning, coronal sections of the thalamus were prepared at E18, and the expression patterns of molecular markers of thalamic nuclei were examined using *in situ* hybridization.

Consistent with the results obtained with Foxp2 (R552H) knockin mice, introduction of Foxp2 shRNA into the thalamic primordium suppressed the expression of *EphA8* and *cadherin-6* (Fig. 10*D*, arrowheads) and increased that of *Gbx2* and *Lhx2* (Fig. 10*E*, arrows), suggesting that Foxp2 shRNA markedly reduced the size of the posterior region of the thalamus, whereas it increased the size of the intermediate region of the thalamus. These results suggest that Foxp2 in the thalamus regulates thalamic patterning.

Foxp2 regulates thalamocortical projection patterns

I next examined if Foxp2 regulates not only gene expression patterns in the thalamus but also thalamocortical projection patterns using the neuronal tracer DiI (Fig. 11*A*). Because the intermediate region of the thalamus projects to the prefrontal cortex [46, 47] and was expanded in Foxp2 (R552H) knockin mice (Figs. 7 and 8), I injected DiI into the prefrontal cortex at P6 and examined if retrogradely labeled DiI-positive areas in the thalamus would be expanded in Foxp2 (R552H) knockin mice (Fig. 11*A*). One day after DiI injection, I made coronal sections of the cerebral cortex and confirmed that DiI was indeed injected into the prefrontal cortex (Fig. 11*B*,*C*,*D*). Then, coronal sections of the thalamus were stained with anti-VGLUT2 antibody using digitonin, which is a detergent suitable for DiI-labeled sections [40]. As expected, I found that DiI-positive retrogradely labeled areas were much larger in Foxp2 (R552H) knockin mice than in wild-type mice (Fig. 11*E*,*F*, arrows). This expanded DiI-positive area seemed to correspond to the expanded *Lhx2*- and *Gbx2*-positive intermediate region of the thalamus (Figs. 7 and 8). These results suggest that Foxp2 regulates not only gene expression patterns in the thalamus but also thalamocortical projection patterns.

As I have shown, the VP was smaller in Foxp2 (R552H) knockin mice (Figs. 6-8). Because the VP contains whisker-related patterns called barreloids [48], I thought it would be

intriguing to examine if barreloid patterns in the VP were affected in Foxp2 (R552H) knockin mice. Coronal sections of the thalamus were subjected to VGLUT2 immunostaining at P7. I found that barreloid patterns were severely disrupted in Foxp2 (R552H) knockin mice (Fig. 12*A*, arrow). Disrupted barreloid patterns in the thalamus led me to examine barrel patterns in the primary somatosensory area (S1) of the cerebral cortex using VGLUT2 immunostaining. I found that barrel patterns were lost in the anterior portion of the postero-medial barrel subfield (PMBSF), the antero-lateral barrel subfield (ALBSF) and the region of S1 corresponding to the forelimb (Fig. 12*B*, arrowheads). This is consistent with the idea that disruption of barreloid patterns in the thalamus leads to disruption of barrel patterns in the cerebral cortex. On the other hand, because Foxp2 is expressed not only in the thalamus but also in other brain regions such as the cerebral cortex and the striatum, and because I used Foxp2 (R552H) global knockin mice for this analysis, it still remains possible that the changes in barrel patterns in the cerebral cortex are mediated by Foxp2 expressed in the other brain regions. It would be important to analyze whether the formation of barrel patterns is indeed regulated by Foxp2 in the thalamus.

I have also shown that the Po in the thalamus was lost in Foxp2 (R552H) knockin mice (Fig. 7). The Po sends thalamocortical axons to septa [49, 50], which are the areas between barrels in layer 4 of S1 in the cerebral cortex. I therefore hypothesized that thalamocortical projections from the Po were decreased, and septa were shrunken in Foxp2 (R552H) knockin mice. Consistent with my hypothesis, VGLUT2 immunostaining of S1 showed that VGLUT2-negative areas between VGLUT2-positive barrels were narrower in Foxp2 (R552H) knockin mice than in wild-type mice (Fig. 12*B*, inset, arrows).

To further confirm thalamocortical projections from the Po really were decreased in Foxp2 (R552H) knockin mice, I injected DiI into S1, where thalamocortical projections from both the VP and the Po were observed in wild type mice (Fig. 13*A*). Two days after DiI injection,

to confirm the location of the DiI-injected area was indeed within S1, I made coronal sections of the cerebral cortex and stained with anti-VGLUT2 antibody using digitonin. VGLUT2 immunohistochemistry showed that DiI-injected side was located in S1, which had VGLUT2-positive barrels (Fig. 13*B*, arrowheads). I then made coronal sections of the thalamus and examined the distribution patterns of retrogradely labeled DiI-positive soma in the thalamus. As expected, DiI-positive areas existed in both the VP and the Po in wild type mice (Fig. 13*C*). In contrast, I found that DiI-positive retrogradely labeled areas in the Po (Fig. 13*C*, arrows) were almost absent in Foxp2 (R552H) knockin mice (Fig. 13*C*, arrowheads), while those in the VB were present (Fig. 13*C, D*). This result suggests that thalamocortical projections from the Po are selectively reduced in Foxp2 (R552H) knockin mice. Taken together with the results of molecular markers, these results indicate that the Po was almost absent in Foxp2 (R552H) knockin mice.

Discussion

I have shown that Foxp2 has a graded expression pattern in the thalamic primordium during development. In Foxp2 (R552H) knockin mice, thalamic nuclei in the posterior region of the thalamus were shrunken, while those in the intermediate region were expanded (Fig. 13*E*). My findings indicate that Foxp2 is crucial for thalamic development.

Foxp2 is a transcription factor regulating thalamic patterning

Although transcription factors distinguishing the thalamic primordium from adjacent brain structures such as the prethalamus, the pretectum and the epithalamus during development have

been intensively investigated [2], transcription factors that regulate patterning inside the thalamus are still largely unclear. My results suggest that Foxp2 is crucial for determining the identities of thalamic nuclei. Previously, the transcription factor Gbx2 was reported to be important for thalamic development. It was reported that Gbx2 suppressed neuronal cell death in a specific subset of thalamic nuclei, and Gbx2 knockout resulted in abnormal arrangements of thalamic nuclei [51]. These results indicate that Foxp2 and Gbx2 play distinct roles in thalamic development. In addition, I also found that thalamic nuclei in the anterior region of the thalamus were not affected in Foxp2 (R552H) knockin mice, raising the possibility that the identities of the anterior region are determined by other transcription factors. Uncovering additional transcription factors regulating thalamic patterning would be an important point for future experiments.

The role of graded expression of Foxp2

My results showed that Foxp2 has a graded expression pattern in the thalamic primordium and that thalamic nuclei in the posterior region of the thalamus were shrunken in Foxp2 (R552H) knockin mice. These results are consistent with the idea that the graded expression pattern of Foxp2 in the thalamic primordium regulates thalamic patterning during development. However, it should be noted that although it is clear that Foxp2 levels determine the characteristics of neurons in the posterior and intermediate regions, I cannot exclude the possibility that, rather than graded expression determining each individual nucleus's identity, certain threshold values of Foxp2 determine regional identity. To address this issue, it is necessary to uncover new molecular markers for the thalamic regions. In this study, I used only 3 kinds of molecular markers, which indicate the anterior, the intermediate and the posterior regions of the thalamus. It is necessary to use many more kinds of molecular markers to divide the thalamus into more than 3 regions. Once such molecular markers are identified, it would be intriguing to examine concentration-dependent

regulation of thalamic patterning by Foxp2.

Foxp2 (R552H) works as a loss-of-function mutation during thalamic development

Previously, it was reported that human FOXP2 (R553H), which corresponds to mouse Foxp2 (R552H), could work as a dominant-negative and suppress not only Foxp2 but also other members of the Foxp subfamily. This report raised the possibility that the changes in thalamic patterning found in Foxp2 (R552H) knockin mice results from inhibition of Foxp proteins other than Foxp2. However, I believe this possibility is unlikely because my knockdown experiments using Foxp2 shRNA showed abnormal thalamic patterning similar to that in Foxp2 (R552H) knockin mice. These results indicate that the thalamic patterning phenotype in Foxp2 (R552H) knockin mice is mediated by Foxp2 itself. However, because I used Foxp2 shRNA in the experiments using molecular markers but not in the experiments in which I looked at projection patterns using DiI, it still remains possible that the changes in the projections of thalamocortical axons are mediated by Foxp proteins other than Foxp2. Therefore, I thought it would be important to analyze whether the projections of thalamocortical axons are also affected by Foxp2 shRNA. Foxp2 knockout mice seemed to be useful for addressing this issue. I therefore obtained Foxp2 knockout mice and tried to analyze their phenotypes. Unfortunately, however, I was not able to analyze Foxp2 knockout mice because newborn pups of Foxp2 knockout mice die soon after birth. This is presumably because while Foxp2 (R552H) may retain some residual functions of Foxp2 [42, 52], a null mutation of Foxp2 leads to lethality soon after birth.

Molecular mechanisms downstream of Foxp2 in thalamic development

To understand the entire picture of the mechanisms underlying thalamic development including thalamic patterning and thalamocortical projections, uncovering the molecular mechanisms

downstream of Foxp2 would be important.

It would be intriguing to investigate whether the molecules that mediate the formation of borders between distinct nuclei in other systems are located downstream of Foxp2 in the thalamus. While Foxp2 has a continuous graded expression pattern in the thalamic primordium early in development, discrete domains of each thalamic nucleus are formed later. Therefore, it seems plausible that the mechanisms downstream of Foxp2 convert continuous changes in the early thalamic primordium into distinct domains of thalamic nuclei. A similar conversion has been well studied in the developing spinal cord [53, 54]. Transcription factors expressed in two adjacent areas in the developing spinal cord comprise a cross-repressive interaction and delineate boundaries between them [55, 56]. Similar mechanisms could be located downstream of Foxp2.

Because thalamocortical projection patterns are affected in Foxp2 (R552H) knockin mice, the expression of axon guidance molecules could be regulated by Foxp2. Although it has been established that ephrin and netrin-1 signaling molecules regulate thalamocortical projection patterns [57, 58], regulatory mechanisms upstream of these axon guidance molecules are still largely unclear. It seems likely that Foxp2 regulates the expressions of the ephrin and/or netrin family member molecules.

Recently, a list of molecules whose expression levels were altered by Foxp2 mutation was identified using DNA microarrays [23]. Although these molecules were identified using brain regions other than the thalamus, they seem to be attractive candidate molecules that could mediate the effects of Foxp2 in thalamic development.

Possible functional phenotypes of the Foxp2-deficient thalamus

Although I have shown the structural changes in the thalamus induced by Foxp2 (R552H) and Foxp2 shRNA, the functional changes in the thalamus are currently unclear. It is well known that

various thalamic nuclei, such as the Po and the VB, play important roles. For example, it was reported that the Po is involved in sensory perception of nociceptive stimuli [59]. Because the Po was almost absent in Foxp2 (R552H) knockin mice, it seems likely that Foxp2 (R552H) knockin mice have abnormal perception of nociceptive stimuli. To address this issue, conditional Foxp2 (R552H) knockin mice, in which Foxp2 (R552H) is expressed only in the thalamus, would be needed because Foxp2 (R552H) knockin mice die by three weeks after birth. A previous study reported a mouse line that expresses Cre only in the thalamus and another mouse line carrying floxed Foxp2 [16, 60], and combining these two mouse lines would be useful for addressing functional changes in the Foxp2-deficient thalamus. Uncovering the structural and functional changes in the Foxp2-deficient thalamus would lead to our comprehensive understanding of the roles of Foxp2 in thalamic development.

Roles of Foxp2 during development

One attractive hypothesis is that FOXP2 is involved in the acquisition of language during evolution. Indeed, FOXP2 is mutated in a monogenic syndrome causing speech and language dysfunction [15]. Furthermore, two amino acid substitutions in the mouse Foxp2 allele, which are found in humans, caused alterations in corticobasal ganglia circuits, indicating that humanized Foxp2 has different functions from mouse Foxp2 [21, 61]. Combined with the fact that the thalamic nucleus pulvinar, which is located in the posterior region of the thalamus and is related to subject's confidence, is observed only in carnivores and primates [62, 63], my finding raised the possibility that the appearance of the pulvinar during evolution was determined by Foxp2. It would be intriguing to examine if mice with humanized Foxp2 have the thalamic structure similar to the pulvinar.

Acknowledgment

I am grateful to Drs. Shoji Tsuji, Takashi Kadowaki and Haruhiko Bito (The University of Tokyo) for their warm support. I thank Kaori Tanno, Yoshie Ichikawa and Mr. Osugi for their assistance and Zachary Blalock for discussions. I also thank all the Kawasaki lab members for their support. I appreciate my parents' warm support. I am sincerely grateful to Dr. Hiroshi Kawasaki (Kanazawa University) for his caring supervision, continuous encouragement and various kinds of support during this study.

References

1 Edward G. Jones. The Thalamus. p 1396-1450. 2007.

2 C. Kiecker and A. Lumsden. The role of organizers in patterning the nervous system. Annu Rev Neurosci. 35:347-367. 2012.

3 E. Puelles, D. Acampora, R. Gogoi, F. Tuorto, A. Papalia, F. Guillemot, S. L. Ang and A. Simeone. Otx2 controls identity and fate of glutamatergic progenitors of the thalamus by repressing GABAergic differentiation. J Neurosci. 26:5955-5964. 2006.

4 E. Robertshaw, K. Matsumoto, A. Lumsden and C. Kiecker. Irx3 and Pax6 establish differential competence for Shh-mediated induction of GABAergic and glutamatergic neurons of the thalamus. Proc Natl Acad Sci U S A. 110:E3919-3926. 2013.

5 M. Chatterjee, Q. Guo, S. Weber, S. Scholpp and J. Y. Li. Pax6 regulates the formation of the habenular nuclei by controlling the temporospatial expression of Shh in the diencephalon in vertebrates. BMC Biol. 12:13. 2014.

6 D. Peukert, S. Weber, A. Lumsden and S. Scholpp. Lhx2 and Lhx9 determine neuronal differentiation and compartition in the caudal forebrain by regulating Wnt signaling. PLoS Biol. 9:e1001218. 2011.

7 T. Hirata, M. Nakazawa, O. Muraoka, R. Nakayama, Y. Suda and M. Hibi. Zinc-finger genes Fez and Fez-like function in the establishment of diencephalon subdivisions. Development. 133:3993-4004. 2006.

8 D. Kobayashi, M. Kobayashi, K. Matsumoto, T. Ogura, M. Nakafuku and K. Shimamura. Early subdivisions in the neural plate define distinct competence for inductive signals. Development. 129:83-93. 2002.

9 M. M. Braun, A. Etheridge, A. Bernard, C. P. Robertson and H. Roelink. Wnt signaling is required at distinct stages of development for the induction of the posterior forebrain. Development. 130:5579-5587. 2003.

10 K. K. Bluske, T. Y. Vue, Y. Kawakami, M. M. Taketo, K. Yoshikawa, J. E. Johnson

and Y. Nakagawa. beta-Catenin signaling specifies progenitor cell identity in parallel with Shh signaling in the developing mammalian thalamus. Development. 139:2692-2702. 2012.

11 Y. Nakagawa and D. D. O'Leary. Combinatorial expression patterns of LIM-homeodomain and other regulatory genes parcellate developing thalamus. J Neurosci. 21:2711-2725. 2001.

12 Y. Nakagawa and D. D. O'Leary. Dynamic patterned expression of orphan nuclear receptor genes RORalpha and RORbeta in developing mouse forebrain. Dev Neurosci. 25:234-244. 2003.

13 K. Yuge, A. Kataoka, A. C. Yoshida, D. Itoh, M. Aggarwal, S. Mori, S. Blackshaw and T. Shimogori. Region-specific gene expression in early postnatal mouse thalamus. J Comp Neurol. 519:544-561. 2010.

14 E. G. Jones and J. L. Rubenstein. Expression of regulatory genes during differentiation of thalamic nuclei in mouse and monkey. J Comp Neurol. 477:55-80. 2004.

15 C. S. Lai, S. E. Fisher, J. A. Hurst, F. Vargha-Khadem and A. P. Monaco. A forkhead-domain gene is mutated in a severe speech and language disorder. Nature. 413:519-523. 2001.

16 S. E. Fisher and C. Scharff. FOXP2 as a molecular window into speech and language. Trends Genet. 25:166-177. 2009.

17 S. C. Vernes, E. Spiteri, J. Nicod, M. Groszer, J. M. Taylor, K. E. Davies, D. H. Geschwind and S. E. Fisher. High-throughput analysis of promoter occupancy reveals direct neural targets of FOXP2, a gene mutated in speech and language disorders. Am J Hum Genet. 81:1232-1250. 2007.

18 E. Spiteri, G. Konopka, G. Coppola, J. Bomar, M. Oldham, J. Ou, S. C. Vernes, S. E. Fisher, B. Ren and D. H. Geschwind. Identification of the transcriptional targets of FOXP2, a gene linked to speech and language, in developing human brain. Am J Hum Genet. 81:1144-1157. 2007.

19 O. J. Lehmann, J. C. Sowden, P. Carlsson, T. Jordan and S. S. Bhattacharya. Fox's in

development and disease. Trends Genet. 19:339-344. 2003.

20 S. Hannenhalli and K. H. Kaestner. The evolution of Fox genes and their role in development and disease. Nat Rev Genet. 10:233-240. 2009.

21 W. Enard, S. Gehre, K. Hammerschmidt, S. M. Holter, T. Blass, M. Somel, M. K. Bruckner, C. Schreiweis, C. Winter, R. Sohr, L. Becker, V. Wiebe, B. Nickel, T. Giger, U. Muller, M. Groszer, T. Adler, A. Aguilar, I. Bolle, J. Calzada-Wack, C. Dalke, N. Ehrhardt, J. Favor, H. Fuchs, V. Gailus-Durner, W. Hans, G. Holzlwimmer, A. Javaheri, S. Kalaydjiev, M. Kallnik, E. Kling, S. Kunder, I. Mossbrugger, B. Naton, I. Racz, B. Rathkolb, J. Rozman, A. Schrewe, D. H. Busch, J. Graw, B. Ivandic, M. Klingenspor, T. Klopstock, M. Ollert, L. Quintanilla-Martinez, H. Schulz, E. Wolf, W. Wurst, A. Zimmer, S. E. Fisher, R. Morgenstern, T. Arendt, M. H. de Angelis, J. Fischer, J. Schwarz and S. Paabo. A humanized version of Foxp2 affects cortico-basal ganglia circuits in mice. Cell. 137:961-971. 2009.

22 C. A. French, X. Jin, T. G. Campbell, E. Gerfen, M. Groszer, S. E. Fisher and R. M. Costa. An aetiological Foxp2 mutation causes aberrant striatal activity and alters plasticity during skill learning. Mol Psychiatry. 17:1077-1085. 2012.

23 E. Fujita, Y. Tanabe, A. Shiota, M. Ueda, K. Suwa, M. Y. Momoi and T. Momoi. Ultrasonic vocalization impairment of Foxp2 (R552H) knockin mice related to speech-language disorder and abnormality of Purkinje cells. Proc Natl Acad Sci U S A. 105:3117-3122. 2008.

24 R. J. Ferland, T. J. Cherry, P. O. Preware, E. E. Morrisey and C. A. Walsh. Characterization of Foxp2 and Foxp1 mRNA and protein in the developing and mature brain. J Comp Neurol. 460:266-279. 2003.

25 S. B. Schulz, S. Haesler, C. Scharff and C. Rochefort. Knockdown of FoxP2 alters spine density in Area X of the zebra finch. Genes Brain Behav. 9:732-740. 2010.

26 M. Groszer, D. A. Keays, R. M. Deacon, J. P. de Bono, S. Prasad-Mulcare, S. Gaub, M. G. Baum, C. A. French, J. Nicod, J. A. Coventry, W. Enard, M. Fray, S. D. Brown, P. M. Nolan, S. Paabo, K. M. Channon, R. M. Costa, J. Eilers, G. Ehret, J. N. Rawlins and

S. E. Fisher. Impaired synaptic plasticity and motor learning in mice with a point mutation implicated in human speech deficits. Curr Biol. 18:354-362. 2008.

27 W. Shu, J. Y. Cho, Y. Jiang, M. Zhang, D. Weisz, G. A. Elder, J. Schmeidler, R. De Gasperi, M. A. Sosa, D. Rabidou, A. C. Santucci, D. Perl, E. Morrisey and J. D. Buxbaum. Altered ultrasonic vocalization in mice with a disruption in the Foxp2 gene. Proc Natl Acad Sci U S A. 102:9643-9648. 2005.

28 Y. C. Chiu, M. Y. Li, Y. H. Liu, J. Y. Ding, J. Y. Yu and T. W. Wang. Foxp2 regulates neuronal differentiation and neuronal subtype specification. Dev Neurobiol. 74:723-738. 2014.

29 S. C. Vernes, P. L. Oliver, E. Spiteri, H. E. Lockstone, R. Puliyadi, J. M. Taylor, J. Ho, C. Mombereau, A. Brewer, E. Lowy, J. Nicod, M. Groszer, D. Baban, N. Sahgal, J. B. Cazier, J. Ragoussis, K. E. Davies, D. H. Geschwind and S. E. Fisher. Foxp2 regulates gene networks implicated in neurite outgrowth in the developing brain. PLoS Genet. 7:e1002145. 2011.

30 K. Sehara, T. Toda, L. Iwai, M. Wakimoto, K. Tanno, Y. Matsubayashi and H. Kawasaki. Whisker-related axonal patterns and plasticity of layer 2/3 neurons in the mouse barrel cortex. J Neurosci. 30:3082-3092. 2010.

31 T. Saito. In vivo electroporation in the embryonic mouse central nervous system. Nat Protoc. 1:1552-1558. 2006.

32 H. Tabata and K. Nakajima. Labeling embryonic mouse central nervous system cells by in utero electroporation. Dev Growth Differ. 50:507-511. 2008.

33 T. Fukuchi-Shimogori and E. A. Grove. Neocortex patterning by the secreted signaling molecule FGF8. Science. 294:1071-1074. 2001.

34 T. Toda, D. Homma, H. Tokuoka, I. Hayakawa, Y. Sugimoto, H. Ichinose and H. Kawasaki. Birth regulates the initiation of sensory map formation through serotonin signaling. Dev Cell. 27:32-46. 2013.

35 H. Kawasaki, J. C. Crowley, F. J. Livesey and L. C. Katz. Molecular organization of the ferret visual thalamus. J Neurosci. 24:9962-9970. 2004.

36 M. Wakimoto, K. Sehara, H. Ebisu, Y. Hoshiba, S. Tsunoda, Y. Ichikawa and H. Kawasaki. Classic Cadherins Mediate Selective Intracortical Circuit Formation in the Mouse Neocortex. Cereb Cortex. 25:3535-3546. 2015.

37 L. Iwai, Y. Ohashi, D. van der List, W. M. Usrey, Y. Miyashita and H. Kawasaki. FoxP2 is a parvocellular-specific transcription factor in the visual thalamus of monkeys and ferrets. Cereb Cortex. 23:2204-2212. 2013.

38 H. Kawasaki, K. Mizuseki, S. Nishikawa, S. Kaneko, Y. Kuwana, S. Nakanishi, S. I. Nishikawa and Y. Sasai. Induction of midbrain dopaminergic neurons from ES cells by stromal cell-derived inducing activity. Neuron. 28:31-40. 2000.

39 S. M. Islam, Y. Shinmyo, T. Okafuji, Y. Su, I. B. Naser, G. Ahmed, S. Zhang, S. Chen, K. Ohta, H. Kiyonari, T. Abe, S. Tanaka, R. Nishinakamura, T. Terashima, T. Kitamura and H. Tanaka. Draxin, a repulsive guidance protein for spinal cord and forebrain commissures. Science. 323:388-393. 2009.

40 Y. Matsubayashi, L. Iwai and H. Kawasaki. Fluorescent double-labeling with carbocyanine neuronal tracing and immunohistochemistry using a cholesterol-specific detergent digitonin. J Neurosci Methods. 174:71-81. 2008.

41 A. Suzuki-Hirano, M. Ogawa, A. Kataoka, A. C. Yoshida, D. Itoh, M. Ueno, S. Blackshaw and T. Shimogori. Dynamic spatiotemporal gene expression in embryonic mouse thalamus. J Comp Neurol. 519:528-543. 2011.

42 S. C. Vernes, J. Nicod, F. M. Elahi, J. A. Coventry, N. Kenny, A. M. Coupe, L. E. Bird, K. E. Davies and S. E. Fisher. Functional genetic analysis of mutations implicated in a human speech and language disorder. Hum Mol Genet. 15:3154-3167. 2006.

43 C. S. Nelson, C. K. Fuller, P. M. Fordyce, A. L. Greninger, H. Li and J. L. DeRisi. Microfluidic affinity and ChIP-seq analyses converge on a conserved FOXP2-binding motif in chimp and human, which enables the detection of evolutionarily novel targets. Nucleic Acids Res. 41:5991-6004. 2013.

44 K. Nakamura, H. Hioki, F. Fujiyama and T. Kaneko. Postnatal changes of vesicular glutamate transporter (VGluT)1 and VGluT2 immunoreactivities and their

colocalization in the mouse forebrain. J Comp Neurol. 492:263-288. 2005.

45 R. Haddad-Tovolli, M. Heide, X. Zhou, S. Blaess and G. Alvarez-Bolado. Mouse thalamic differentiation: gli-dependent pattern and gli-independent prepattern. Front Neurosci. 6:27. 2012.

46 F. Conde, E. Maire-Lepoivre, E. Audinat and F. Crepel. Afferent connections of the medial frontal cortex of the rat. II. Cortical and subcortical afferents. J Comp Neurol. 352:567-593. 1995.

47 W. B. Hoover and R. P. Vertes. Anatomical analysis of afferent projections to the medial prefrontal cortex in the rat. Brain Struct Funct. 212:149-179. 2007.

48 H. Van Der Loos. Barreloids in mouse somatosensory thalamus. Neurosci Lett. 2:1-6. 1976.

49 K. D. Alloway. Information processing streams in rodent barrel cortex: the differential functions of barrel and septal circuits. Cereb Cortex. 18:979-989. 2008.

50 K. Sehara and H. Kawasaki. Neuronal circuits with whisker-related patterns. Mol Neurobiol. 43:155-162. 2011.

51 N. E. Szabo, T. Zhao, X. Zhou and G. Alvarez-Bolado. The role of Sonic hedgehog of neural origin in thalamic differentiation in the mouse. J Neurosci. 29:2453-2466. 2009.

52 H. A. Bruce and R. L. Margolis. FOXP2: novel exons, splice variants, and CAG repeat length stability. Hum Genet. 111:136-144. 2002.

53 J. Briscoe and J. Ericson. Specification of neuronal fates in the ventral neural tube. Curr Opin Neurobiol. 11:43-49. 2001.

54 E. Dessaud, A. P. McMahon and J. Briscoe. Pattern formation in the vertebrate neural tube: a sonic hedgehog morphogen-regulated transcriptional network. Development. 135:2489-2503. 2008.

55 J. Ericson, P. Rashbass, A. Schedl, S. Brenner-Morton, A. Kawakami, V. van Heyningen, T. M. Jessell and J. Briscoe. Pax6 controls progenitor cell identity and neuronal fate in response to graded Shh signaling. Cell. 90:169-180. 1997.

56 J. Briscoe, L. Sussel, P. Serup, D. Hartigan-O'Connor, T. M. Jessell, J. L. Rubenstein

and J. Ericson. Homeobox gene Nkx2.2 and specification of neuronal identity by graded Sonic hedgehog signalling. Nature. 398:622-627. 1999.

57 A. Dufour, J. Seibt, L. Passante, V. Depaepe, T. Ciossek, J. Frisen, K. Kullander, J. G. Flanagan, F. Polleux and P. Vanderhaeghen. Area specificity and topography of thalamocortical projections are controlled by ephrin/Eph genes. Neuron. 39:453-465. 2003.

58 A. W. Powell, T. Sassa, Y. Wu, M. Tessier-Lavigne and F. Polleux. Topography of thalamic projections requires attractive and repulsive functions of Netrin-1 in the ventral telencephalon. PLoS Biol. 6:e116. 2008.

59 L. Frangeul, C. Porrero, M. Garcia-Amado, B. Maimone, M. Maniglier, F. Clasca and D. Jabaudon. Specific activation of the paralemniscal pathway during nociception. Eur J Neurosci. 39:1455-1464. 2014.

60 K. Li, J. Zhang and J. Y. Li. Gbx2 plays an essential but transient role in the formation of thalamic nuclei. PLoS One. 7:e47111. 2012.

61 S. Reimers-Kipping, W. Hevers, S. Paabo and W. Enard. Humanized Foxp2 specifically affects cortico-basal ganglia circuits. Neuroscience. 175:75-84. 2011.

62 Jon H Kaas. Evolution of Nervous Systems. p 517-523. 2007.

63 Y. Komura, A. Nikkuni, N. Hirashima, T. Uetake and A. Miyamoto. Responses of pulvinar neurons reflect a subject's confidence in visual categorization. Nat Neurosci. 16:749-755. 2013.

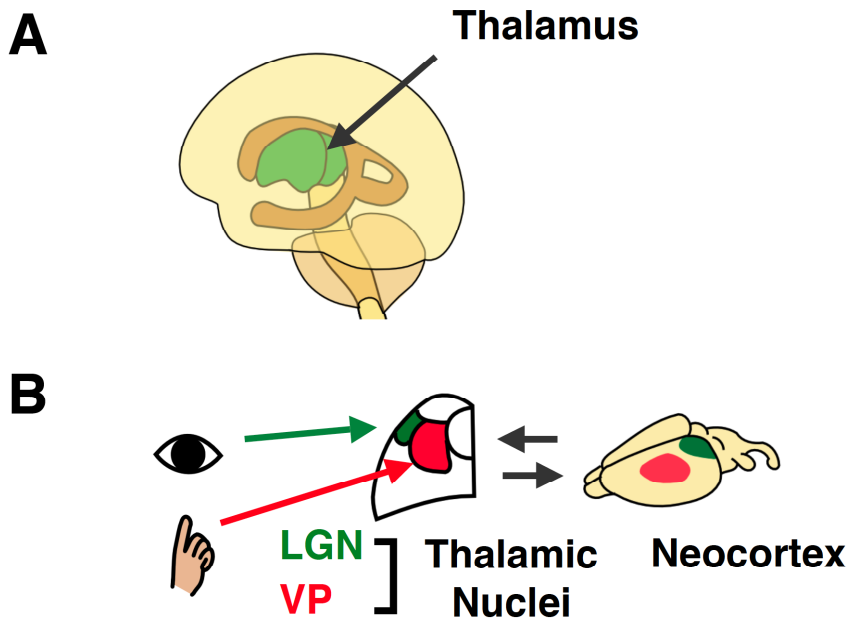

Figure 1. The thalamus in the brain.
(*A*) Schematic organization of the position of the thalamus in the human brain. The thalamus is located deep in the brain and plays critical roles as a relay center of sensory information in the brain. Most sensory information from the periphery is transmitted to the primary sensory areas in the cerebral cortex through the thalamus. (*B*) The thalamus consists of many structurally and functionally segregated thalamic nuclei. Each sensory system (with the exception of the olfactory system) has a corresponding thalamic nucleus that receives its own sensory signals and sends them to the related cortical area. For example, the lateral geniculate nucleus (LGN) relays visual information from the retina to the primary visual cortex (green), and the ventral posterior nucleus (VP) sends somatosensory information to the primary somatosensory cortex (red).

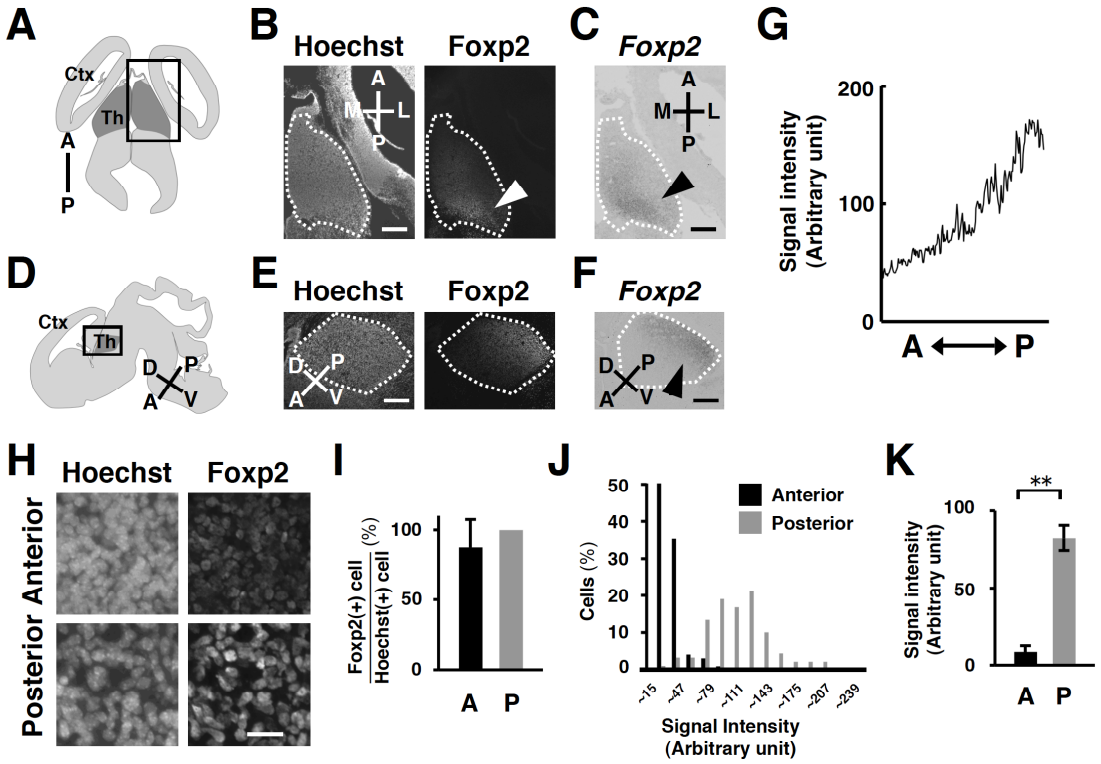

Figure 2. Expression patterns of Foxp2 in the thalamic primordium of the mouse embryo. (*A*) Schematic organization of horizontal sections of the embryonic mouse brain. Images within the box are shown in (*B*) and (*C*). Ctx, cerebral cortex; Th, thalamic primordium. (*B*) Foxp2 immunohistochemistry using horizontal sections of mouse thalamic primordium at E14.5. The areas within the broken lines are the thalamic primordium. Note that Foxp2 was abundantly expressed in the posterior region (arrowhead) but almost absent in the anterior region of the thalamic primordium. (*C*) *In situ* hybridization using horizontal sections of mouse thalamic primordium at E14.5. *Foxp2* mRNA was also abundantly expressed in the posterior region of the thalamic primordium (arrowhead). (*D*) Schematic organization of sagittal sections of the embryonic mouse brain. Images within the box are shown in (*E*) and (*F*). Ctx, cerebral cortex; Th, thalamic primordium. (*E*) Foxp2 immunohistochemistry using sagittal sections of mouse thalamic primordium at E14.5. The areas within the broken lines are the thalamic primordium. (*F*) *In situ* hybridization using sagittal sections of mouse thalamic primordium at E14.5. *Foxp2* mRNA was abundantly expressed in the posterior region of the thalamic primordium (arrowhead). (*G*) A representative densitometry scan along the anterior (A) to posterior (P) axis of the thalamic primordium in horizontal sections at E14.5. (*H*) Higher-magnification images of Foxp2 immunohistochemistry of the thalamic primordium. (*I*) The percentages of Foxp2-positive cells. The numbers of Foxp2-positive cells in the anterior region (A) and the posterior region (P) were counted and divided by those of Hoechst-positive cells. Note that almost all cells were Foxp2-positive in both anterior and posterior regions. An error bar indicates

SD. (*J*) Histogram of Foxp2 expression level in each cell in the anterior region and the posterior region of the thalamic primordium. Note that most cells in the anterior region had very low Foxp2 expression levels. (*K*) Average Foxp2 signal intensity in the anterior region (A) was lower than that in the posterior region (P) of the thalamic primordium. ** $p < 0.01$, two-sided Welch's t-test. Error bars indicate SEM. A, anterior; P, posterior; L, lateral; M, medial; D, dorsal; V, ventral. Scale bars = 250 μm (*B*, *C*, *E*, *F*) and 20 μm (*H*).

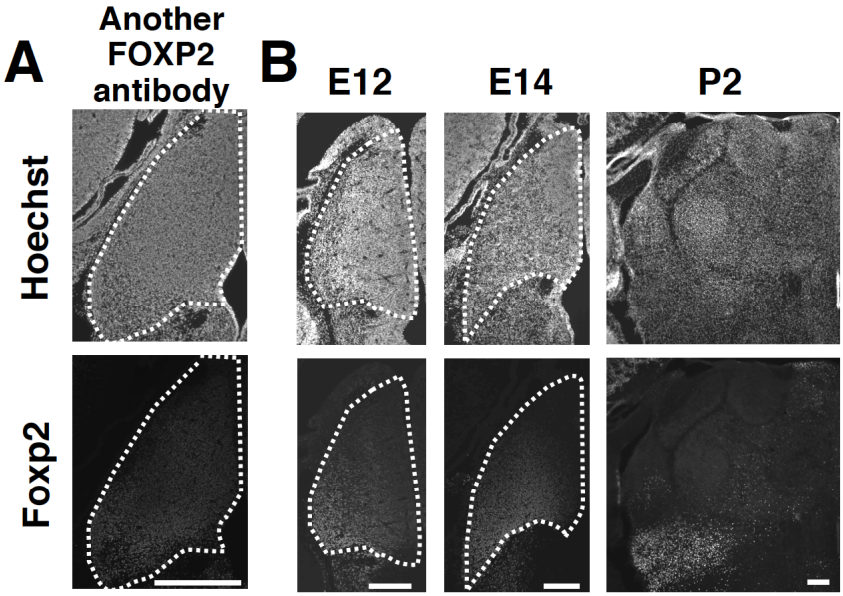

Figure 3. Time course of Foxp2 expression.

(*A*) Immunohistochemistry using another anti-FOXP2 antibody also showed a graded expression pattern of Foxp2 in a horizontal section of the thalamic primordium at E14. (*B*) The expression patterns of Foxp2 protein were analyzed at E12, E14 and P2. The graded patterns were found in horizontal sections of the thalamic primordium at E12 and E14, whereas the graded expression of Foxp2 was almost absent at P2. Scale bars = 500 μm (*A*) and 200 μm (*B*).

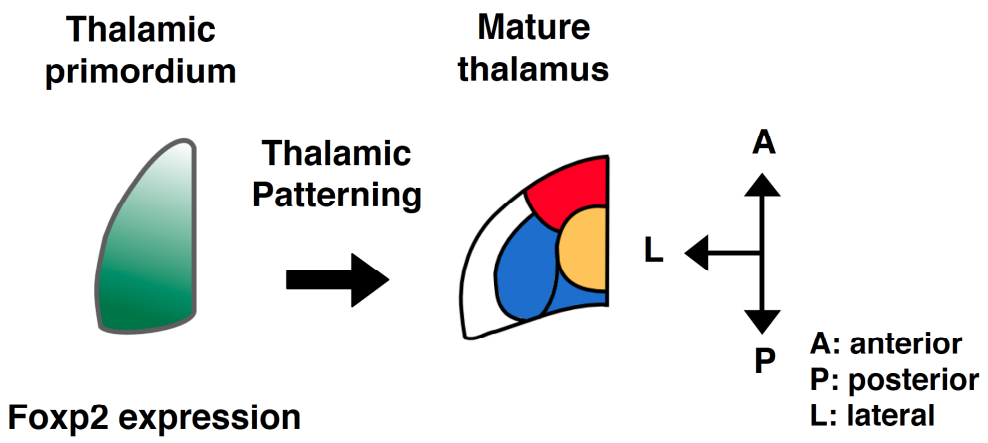

Figure 4. My hypothesis about the role of Foxp2 in the thalamic development.
(Left) Schematic organization of the thalamic primordium at E14. Foxp2 shows the graded expression pattern in the thalamic primordium. Foxp2 expression levels were highest in the posterior region, lower in the intermediate region, and lowest in the anterior region of the thalamic primordium. (Right) Schematic organization of the mature thalamus at P2. Each thalamic nucleus is well segregated. Red, the anterior region of the thalamus; yellow, the intermediate region of the thalamus; blue, the posterior region of the thalamus. The graded expression pattern of Foxp2 in the thalamic primordium leads me to hypothesize that Foxp2 regulates thalamic patterning.

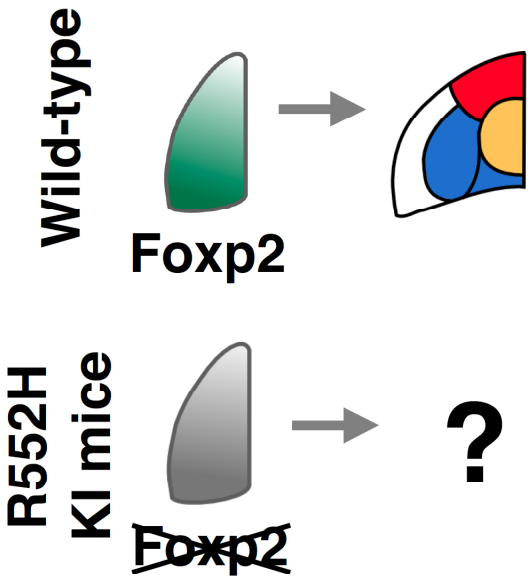

Figure 5. My experimental plan.
To examine the role of Foxp2 in thalamic patterning, I utilized Foxp2 (R552H) knockin mice that have a missense loss-of-function mutation in the forkhead domain of Foxp2. This mutation disrupts the DNA binding and transactivation properties of Foxp2 protein. I examined the thalamic patterning in Foxp2 (R552H) knockin mice.

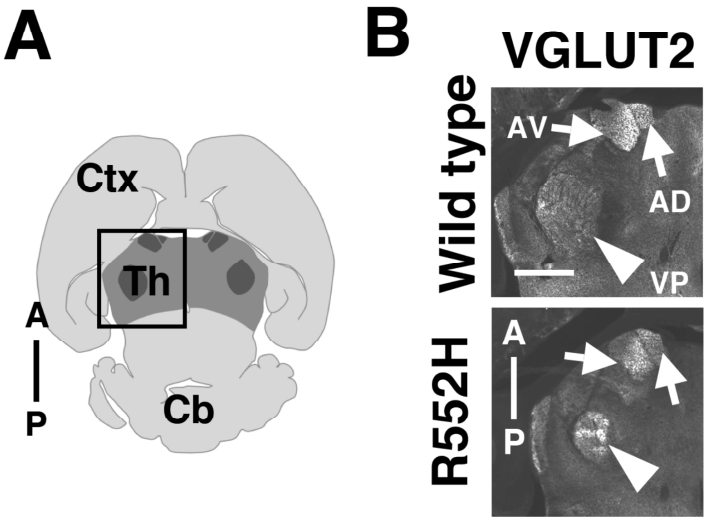

Figure 6. The VP is smaller in Foxp2 (R552H) knockin mice.
(*A*) Schematic organization of horizontal sections of the mouse brain at P7. Images within the box are shown in (*B*). Ctx, cerebral cortex; Th, Thalamus; Cb, cerebellum. (*B*) VGLUT2 immunohistochemistry using horizontal sections of the thalamus of Foxp2 (R552H) knockin mice at P7. The ventral posterior nucleus (VP) in the thalamus was smaller in Foxp2 (R552H) knockin mice (arrowheads). A, anterior; P, posterior. AD, the anterodorsal nucleus; AV, the anteroventral nucleus; VP, the ventral posterior nucleus. Scale bar = 1 mm.

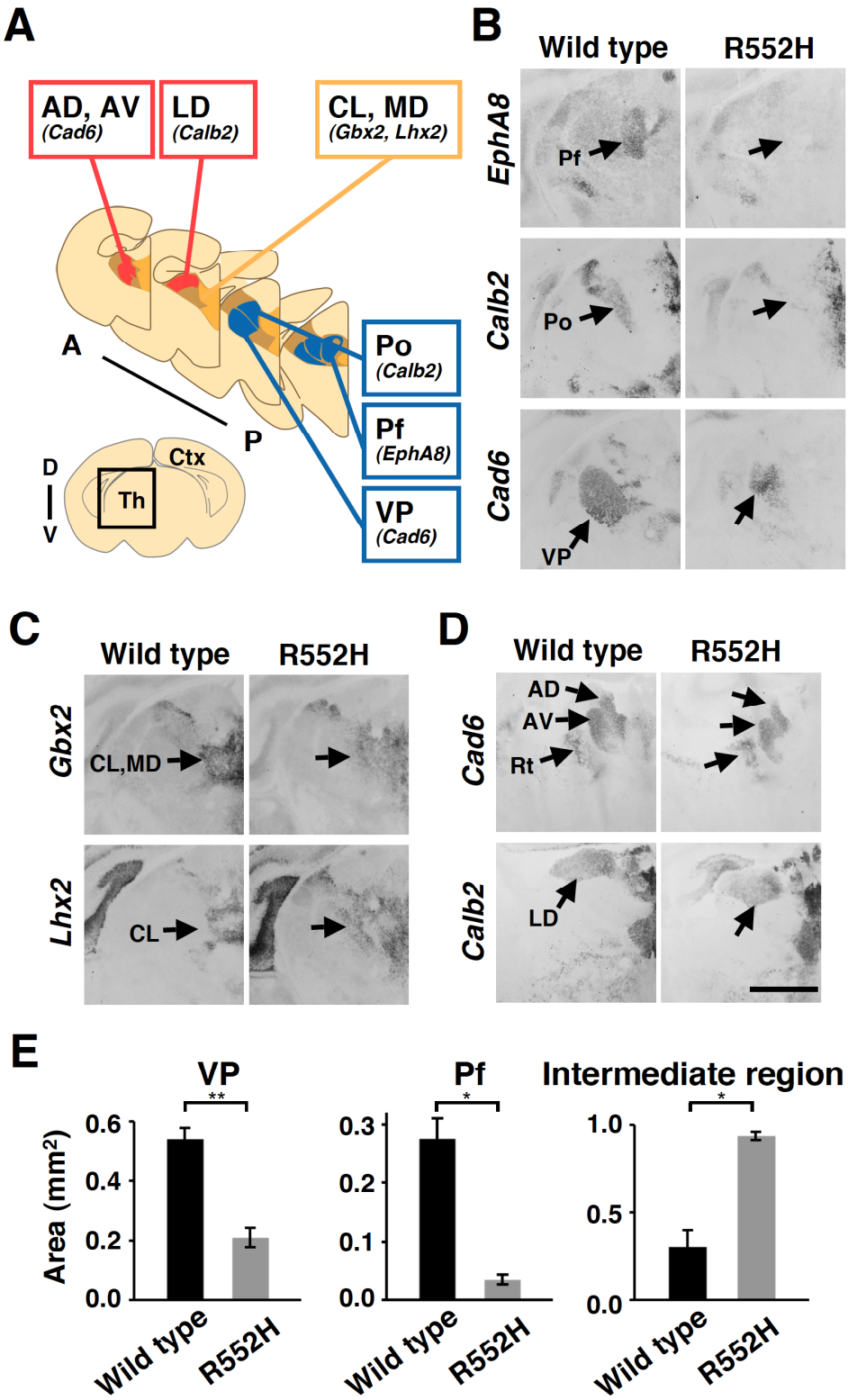
A
AD, AV
(Cad6)
LD
(Calb2)
CL, MD
(Gbx2, Lhx2)
Po
(Calb2)
Pf
(EphA8)
VP
(Cad6)
A
P
D
V
Ctx
Th
B
Wild type
R552H
EphA8
Pf
Calb2
Po
Cad6
VP
C
Wild type
R552H
Gbx2
CL,MD
Lhx2
CL
D
Wild type
R552H
Cad6
AD
AV
Rt
Calb2
LD
E
VP
Pf
Intermediate region
Area (mm²)
0.6
0.4
0.2
0.0
0.3
0.2
0.1
0.0
1.0
0.5
0.0
**
*
*
Wild type
R552H
Wild type
R552H
Wild type
R552H

Figure 7. The identities of thalamic nuclei in coronal sections of Foxp2 (R552H) knockin mice.

(*A*) Schematic organization of coronal sections of the mouse brain. Coronal sections were prepared from Foxp2 (R552H) knockin mice at P2, and were examined using *in situ* hybridization. Marker expressions in the thalamic nuclei are shown in the upper panel. Images within the box of the lower panel are shown in (*B*), (*C*) and (*D*). Ctx, cerebral cortex; Th, thalamus. A, anterior; P, posterior; D, dorsal; V, ventral. (*B*) The posterior region of the thalamus. *EphA8* is expressed in the parafascicular nucleus (Pf), and *calbindin 2* (*Calb2*) is expressed in the posterior nucleus (Po). *Cadherin-6* (*Cad6*) is expressed in the VP. Note that the Pf, the Po, and the VP were markedly smaller in Foxp2 (R552H) knockin mice (arrows). (*C*) The intermediate region of the thalamus. *Lhx2* is expressed in the central lateral nucleus (CL), and *Gbx2* is expressed in the CL and the mediodorsal nucleus (MD). Note that the CL and the MD were larger in Foxp2 (R552H) knockin mice (arrows). (*D*) The anterior region of the thalamus. *Cad6* is expressed in the anterodorsal nucleus (AD), the anteroventral nucleus (AV) and the reticular nucleus (Rt). *Calb2* is expressed in the lateral dorsal nucleus (LD). The sizes of the AD, the AV, the Rt and the LD were unaffected (arrows). Scale bar = 1 mm. (*E*) Quantitative analysis of the effects of Foxp2 (R552H) on the sizes of thalamic nuclei. The sizes of the VB and the Pf were significantly smaller, and the size of the intermediate region was significantly larger in Foxp2 (R552H) knockin mice. ** $p < 0.01$, * $p < 0.05$, two-sided Welch's t-test. Error bars indicate SEM. n=3 pups for control, 3 pups for Foxp2 (R552H) knockin mice.

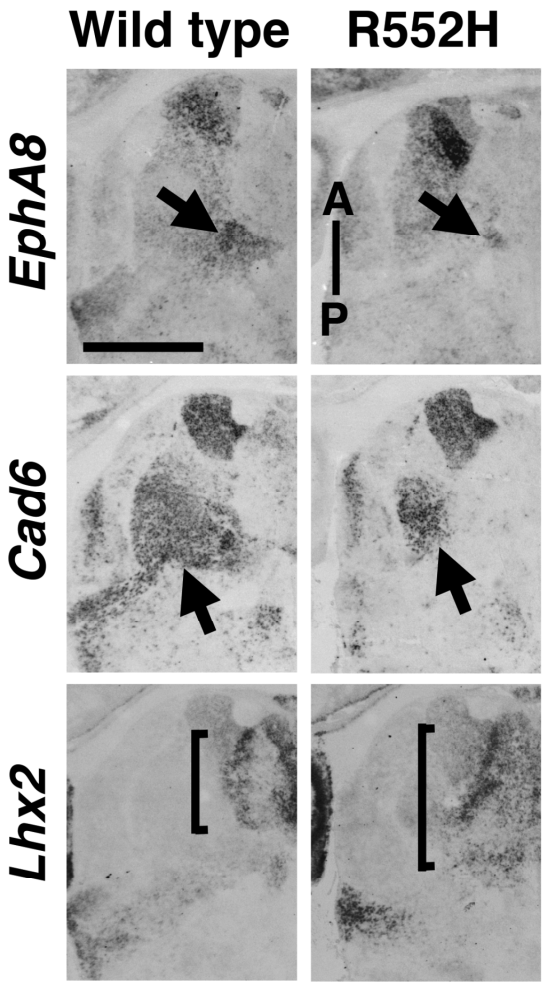

Figure 8. The changes of thalamic nuclei in horizontal sections of Foxp2 (R552H) knockin mice.

Horizontal sections of the thalamus were prepared from Foxp2 (R552H) knockin mice at P2, and were examined using *in situ* hybridization. Note that the *Lhx2*-positive area was expanded posteriorly in Foxp2 (R552H) knockin mice (square brackets), while *EphA8*- and *cadherin-6*-positive areas were shrunken (arrows). A, anterior; P, posterior. Scale bar = 2 mm.

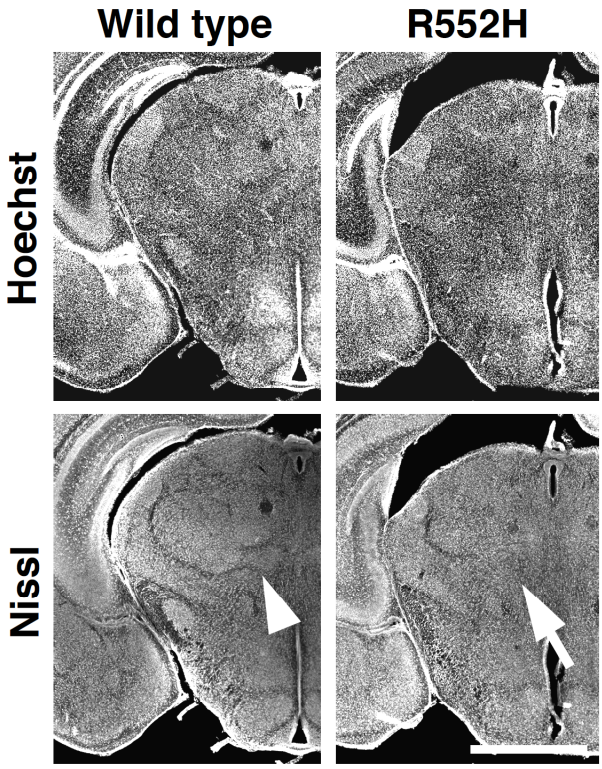

Figure 9. Cytoarchitectonic structures of thalamic nuclei were obscure in Foxp2 (R552H) knockin mice.

Coronal sections of the thalamus at P7 were subjected to Hoechst 33342 and Nissl staining. In the thalamus of wild type mice, thalamic nuclei were well segregated, and borders between thalamic nuclei were clearly visible (arrowhead). In contrast, borders between thalamic nuclei became obscure in Foxp2 (R552H) knockin mice (arrow). Scale bar = 2 mm.

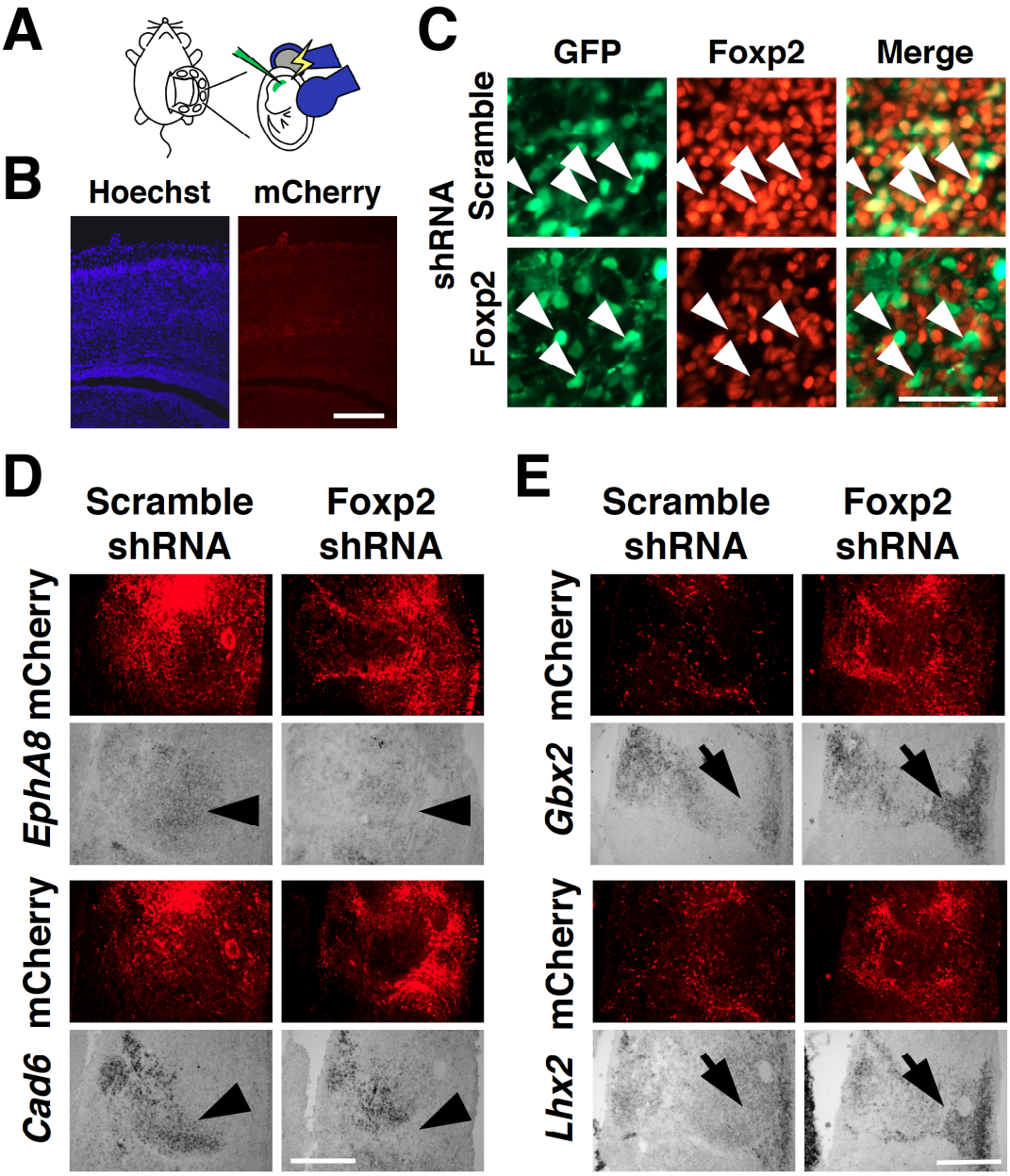

Figure 10. Foxp2 knockdown in the thalamus changed thalamic patterning.
(*A*) Experimental procedure for *in utero* electroporation to investigate the role of Foxp2 within the thalamus. pCAG-mCherry (0.2 mg/mL) and pSUPER-Foxp2-shRNA (0.8 mg/mL) were co-transfected into the thalamic primordium using *in utero* electroporation at E11, and coronal sections were prepared at E14 and E18. (*B*) Images of the cerebral cortex. Note that no mCherry-positive transfected cells were found in the cerebral cortex. (*C*) Foxp2 immunostaining at E14. Note that Foxp2 immunoreactivity was markedly suppressed by Foxp2 shRNA. (*D*) Expression patterns of *EphA8* and *Cad6* visualized with *in situ* hybridization. (*E*) Expression patterns of *Gbx2* and *Lhx2* visualized with *in situ* hybridization. Scale bars = 200 μm (*B*), 50 μm (*C*) and 500 μm (*D, E*).

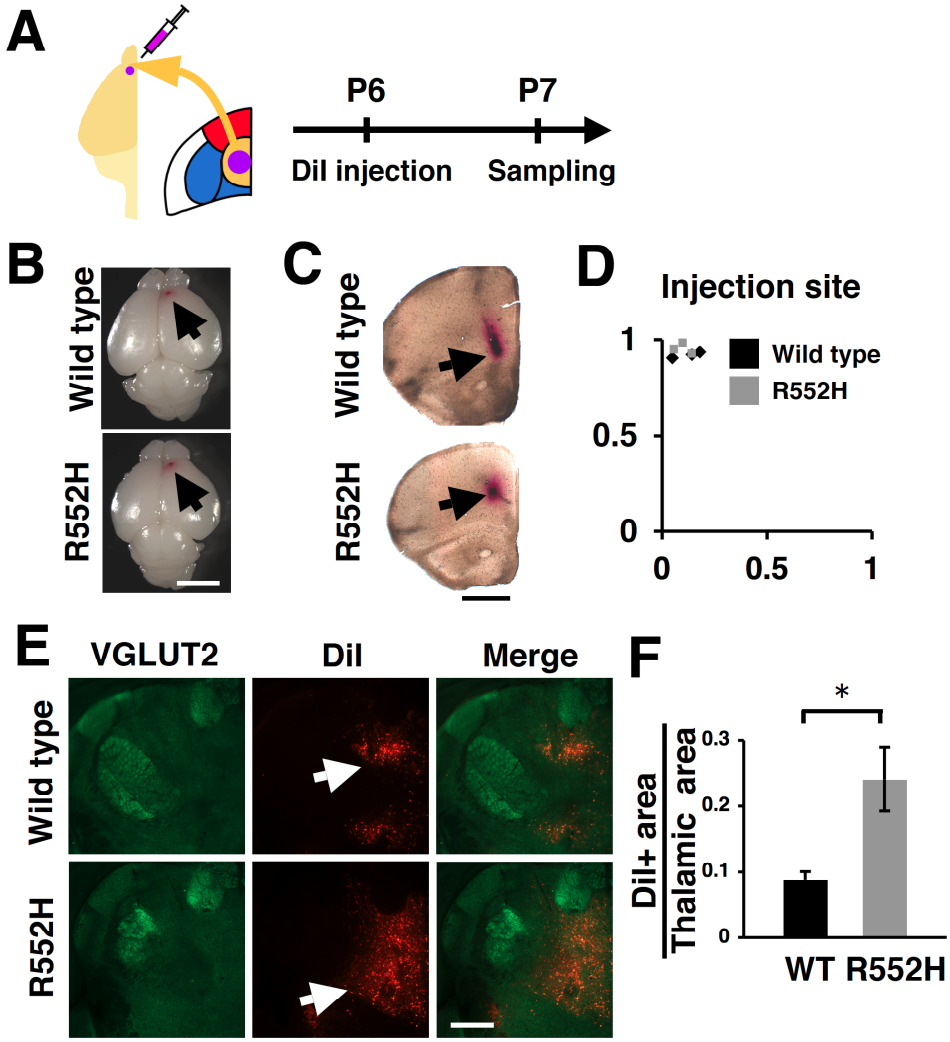

Figure 11. Thalamocortical projections from the intermediate region in Foxp2 (R552H) knockin mice.

(*A*) Experimental design. Thalamic neurons projecting to the prefrontal cortex were retrogradely labeled with DiI (left, purple). DiI was injected into the prefrontal cortex at P6 (purple), and coronal sections were prepared at P7 (right). (*B*) Dorsal views of DiI-injected brains. DiI-injected areas are indicated by arrows. (*C*) Coronal sections of the prefrontal cortex. The injection sites of DiI solutions were visible (arrows). (*D*) The distribution of the positions of DiI-injected sites in wild type mice (black) and Foxp2 (R552H) knockin mice (gray). Each dot represents the position of DiI injection site of one mouse. (*E*) Coronal sections of the thalamus stained with anti-VGLUT2 antibody. Thalamic neurons projecting to the prefrontal cortex were retrogradely labeled with DiI. Note that many DiI-positive neurons were observed in Foxp2 (R552H) knockin mice (arrows). (*F*) The sizes of retrogradely-labeled DiI-positive area in the thalamus. The size of DiI-positive area was significantly larger in Foxp2 (R552H) knockin mice than in wild type mice. * $p < 0.05$, two-sided Student's t-test. Error bars indicate SEM. n=3 pups for control, 3 pups for Foxp2 (R552H) knockin mice. Scale bars = 3 mm (*B*), 1 mm (*C*) and 500 μm (*E*).

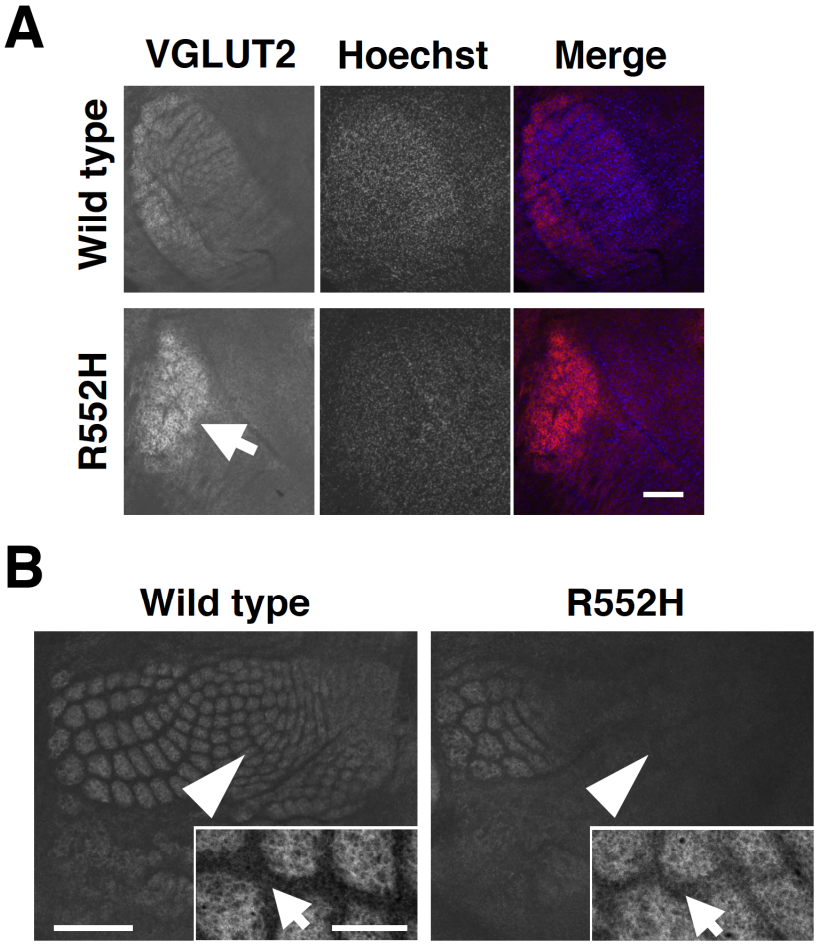

Figure 12. Abnormal organization of barreloids in the thalamus and barrels in the cerebral cortex.

(*A*) Coronal sections of the thalamus were prepared at P7 and stained with anti-VGLUT2 antibody to visualize whisker-related patterns of barreloids in the VP of the thalamus. While barreloids were well segregated in control mice, they were disrupted in Foxp2 (R552H) knockin mice (arrow). (*B*) Tangential sections were prepared from the flattened cerebral cortex and were stained with anti-VGLUT2 antibody to visualize barrel patterns in S1. While barrel patterns were clearly visible in control mice, clear barrel patterns were lost in the majority of S1 in Foxp2 (R552H) knockin mice (arrowheads). Magnified images are shown in the insets. Note that VGLUT2-negative septa (arrows) are narrower in Foxp2 (R552H) knockin mice. Scale bars = 200 μm (*A*), 1 mm (*B*), 200 μm (*B*, inset).

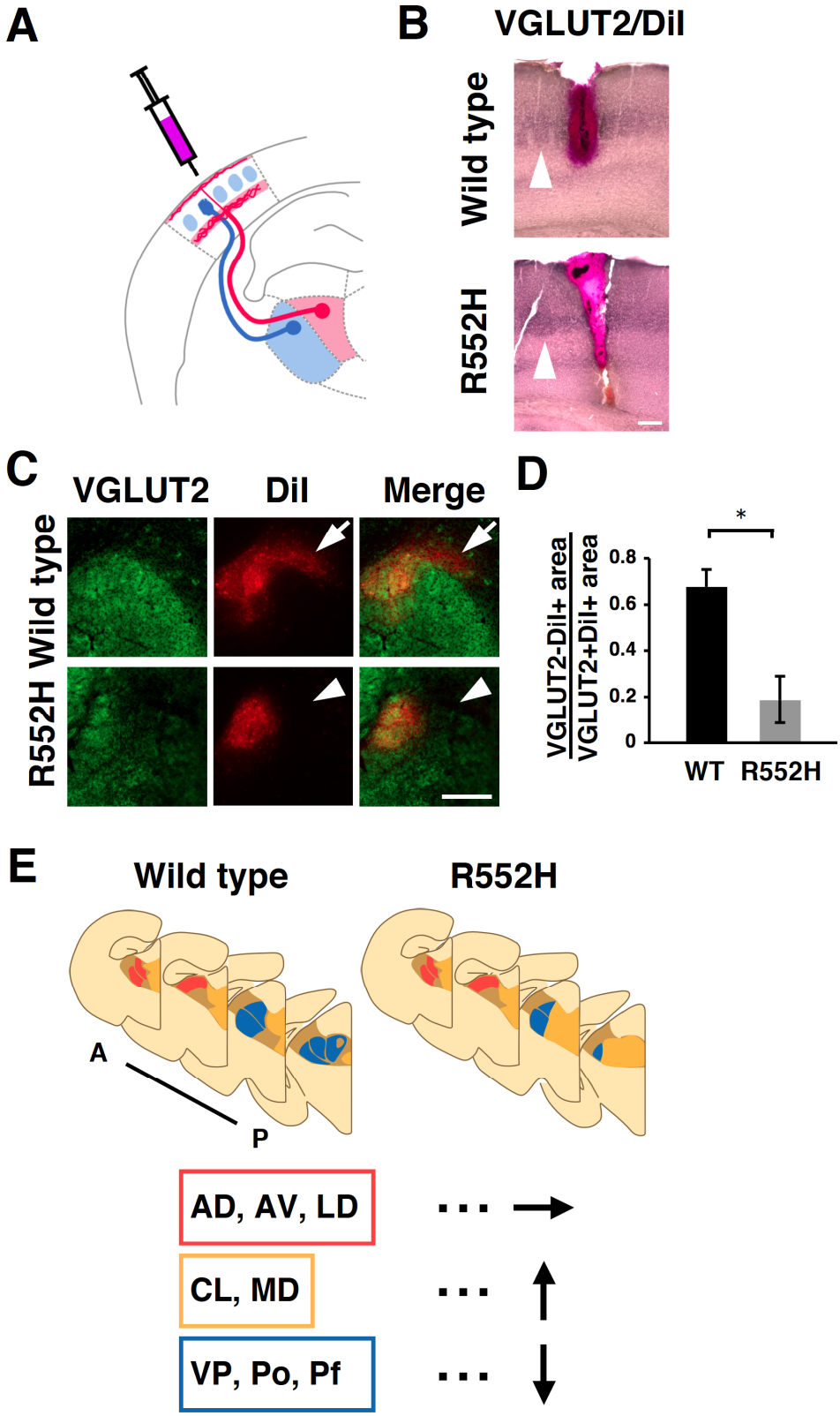
A
B
VGLUT2/DiI
Wild type
R552H
C
VGLUT2
DiI
Merge
Wild type
R552H
D
VGLUT2-DiI+ area
VGLUT2+DiI+ area
0.8
0.6
0.4
0.2
0
*
WT
R552H
E
Wild type
R552H
A
P
AD, AV, LD
CL, MD
VP, Po, Pf

Figure 13. Thalamocortical projections from the Po and the VP in Foxp2 (R552H) knockin mice.

(*A*) Experimental design. To retrogradely label thalamic neurons projecting to S1, DiI was injected into S1 at P13 (purple), and coronal sections were prepared at P15. Red, thalamocortical projection from the Po; blue, thalamocortical projection from the VP. (*B*) Coronal sections of DiI-injected areas stained with anti-VGLUT2 antibody. Note that DiI-positive areas were located within S1, which has barrels (arrowheads). (*C*) Coronal sections of the thalamus stained with anti-VGLUT2 antibody, which strongly labeled the VP. The VP was retrogradely labeled with DiI both in control and Foxp2 (R552H) knockin mice, suggesting that DiI was successfully injected into S1. Note that DiI signal in the Po of wild type mice (arrows) was lost in Foxp2 (R552H) knockin mice (arrowheads). (*D*) The sizes of DiI-positive/VGLUT2-negative area divided by DiI-positive/VGLUT2-positive area. * $p < 0.05$, two-sided Welch's t-test. Error bars indicate SEM. n=3 pups for control, 3 pups for Foxp2 (R552H) knockin mice. (*E*) Schematic organization of coronal sections of the thalamus in wild type and Foxp2 (R552H) knockin mice. Thalamic nuclei in the posterior region of the thalamus (blue) are shrunken in Foxp2 (R552H) knockin mice, whereas thalamic nuclei in the intermediate region are expanded (yellow). Thalamic nuclei in the anterior region of the thalamus (red) are not affected in Foxp2 (R552H) knockin mice. A, anterior; P, posterior. Scale bars = 200 μm (*B*), and 400 μm (*C*).